Fisheries Research 272 (2024) 106927

Contents lists available at ScienceDirect

Fisheries Research

journal homepage: www.elsevier.com/locate/fishres

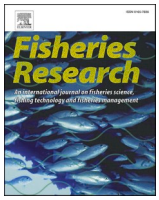

Otolith morphometry and Fourier transform near-infrared (FT-NIR) spectroscopy as tools to discriminate archived otoliths of newly detected cryptic species, *Etelis carbunculus* and *Etelis boweni*

Kristen Dahl [a,*,1], Joseph O'Malley [a], Beverly Barnett [b], Bill Kline [b], Joseph Widdrington [c]

[a] National Marine Fisheries Service, Pacific Islands Fisheries Science Center, NOAA, 1845 Wasp Boulevard, Building 176, Honolulu, HI 96818, USA
[b] Panama City Laboratory, National Marine Fisheries Service, Southeast Fisheries Science Center, NOAA, 3500 Delwood Beach Road, Panama City, FL 32408, USA
[c] Southern Seas Ecology Laboratories, School of Biological Sciences, University of Adelaide, North Terrace, South Australia 5005, Australia

ARTICLE INFO

Keywords:
Cryptic species
Otolith morphology
Morphometrics
Fisheries
FT-NIR spectroscopy

ABSTRACT

Cryptic speciation was recently verified in *Etelis carbunculus*, an important component of federally managed bottomfish fisheries in the Pacific Territories of the United States. As a result, archived otolith collections used for fishery assessment are now contaminated with newly described *E. boweni* in areas where these species co-occur. We compared the efficacy of otolith morphometrics and Fourier transform near-infrared (FT-NIR) spectroscopy to discriminate species first using voucher (i.e., known species) otoliths (n = 93) from the SW Pacific, then applied optimal models to archived otoliths (n = 91) collected around Guam. Significant and distinguishable differences in otolith morphometrics as well as FT-NIR spectral absorbance patterns were observed between *E. carbunculus* and *E. boweni* voucher samples. Classification models applied using both morphometric measurements (quadratic discriminant analysis) and FT-NIR spectral data (partial least squares discriminant analysis) were able to predict species with a high (93 – 100%) degree of accuracy despite a relatively large spatial area of specimen collection (± 10° latitude and longitude) and regardless of whether otoliths were whole (i.e., unbroken). Further, each method identified members of newly described *E. boweni* in the archived collection of *E. carbunculus* otoliths captured around Guam, providing strong evidence that the species' distributions overlap in this region. The purported identification of both *E. carbunculus* and *E. boweni* in the archived catch from Guam has important implications for fisheries management; therefore, it is imperative that the corresponding otolith collections are examined to ensure that the otoliths are assigned to the correct species.

1. Introduction and Rationale

Eteline snappers (subfamily Etelinae) are part of the bottomfish management unit species (BMUS) that are federally managed in the United States Pacific Territories of American Samoa, Guam, and the Commonwealth of the Northern Mariana Islands (CNMI). The Pacific Islands Fisheries Science Center (PIFSC) within the National Oceanic and Atmospheric Administration (NOAA) is responsible for providing the life history information which is necessary for quantitative stock assessments on these species. The collection of otoliths, accomplished via fisheries independent research cruises and fisheries dependent territorial commercial fishery biosampling programs in this region, is required for BMUS life history research and the estimation of length-at-age and growth.

Etelis carbunculus Cuvier (Cuvier and Valenciennes, 1828) is an important component of the BMUS fisheries in the Pacific Territories of the United States (Langseth et al., 2019). There has long been speculation about whether *E. carbunculus* actually comprises two species due to its extensive range from Seychelles (western Indian Ocean) to Hawai'i, and geographic variation in certain morphological characters, such as maximum body size, growth, and otolith morphology (Anderson, 1981; Smith and Kostlan, 1991; Wakefield et al., 2014; Williams et al., 2015). Historically, *E. carbunculus* was divided into *E. carbunculus* (Seychelles holotype 1828) and *E. marshi* (Hawaii holotype), but *E. marshi* was later designated as a junior synonym (i.e., a previously published name) of *E. carbunculus*, and not a unique species (Anderson, 1981). Later,

* Corresponding author.
E-mail address: kristen.dahl@noaa.gov (K. Dahl).
[1] ORCID: 0000–0003-4939–1084

https://doi.org/10.1016/j.fishres.2023.106927
Received 4 October 2023; Received in revised form 19 December 2023; Accepted 20 December 2023
Available online 4 January 2024

phenotypic differences in otolith morphology of *E. carbunculus* reported from different regions ignited a new debate around the possibility of a cryptic species pair (Smith, 1992; Smith and Kostlan, 1991). Recent genetic and morphological studies have provided conclusive evidence that *Etelis carbunculus* comprises two cryptic species, *E. carbunculus*, the pygmy ruby snapper, and *E. boweni*, the newly described giant ruby snapper (Andrews et al., 2021; Andrews et al., 2016; Loeun et al., 2014). Although exceptionally similar in their morphology, the two species differ in coloration of the dorsal caudal fin tip and the shape of the opercular spine (Andrews et al., 2016).

Now that taxonomic revision of the species complex has been verified, life history research has revealed fundamental differences in the biology between *E. carbunculus* and *E. boweni*, including maximum body size, growth rates, and length at age (Wakefield et al., 2020; Williams et al., 2017). Due to their overlapping distributions across the Indo-Pacific, both species have been previously misreported as a single species (*E. carbunculus*) in fisheries catch data and in biological studies (Wakefield et al., 2020; Williams et al., 2013). This complicates life history research, because the otolith collections that were thought to be solely *E. carbunculus* are now known to be contaminated with an unknown number of *E. boweni* otoliths. Collections of biological samples on these species for which misidentification is a potential issue go back decades, and fisheries age-structured assessments that incorporate life history data from the cryptic species alongside *E. carbunculus* may suffer from model misspecification. This is also true for data poor assessment approaches that rely heavily on otolith-derived growth estimates. Given the inherent vulnerability of Eteline snappers to overexploitation (Williams et al., 2013), it is imperative that methods be developed to recognize speciation within archived otolith collections to move forward with sustainable management. Historical fish life history collections might not have any other specimens available (e.g., tissue, whole animals) besides otoliths with which to verify species identification.

The same issue with *E. carbunculus* otoliths was encountered by Wakefield et al. (2014) from collections made in the eastern Indian Ocean and South Pacific Ocean (though it should be noted that, in their manuscript, they used the now-invalid species name *E. marshi* for *E. carbunculus*, and *E. carbunculus* for *E. boweni*). Researchers used otolith morphology information (length, width, thickness, and weight) in a canonical discrimination analysis approach to distinguish between *E. carbunculus* and *E. boweni* otoliths, which was found to be reliable (Wakefield et al., 2014). Compared to digital shape analysis with Fourier harmonic descriptors, Wakefield et al. (2014) argued that a simplistic morphometric approach using these caliper-derived measurements was rapid, efficient, and effective in determining species identification. However, this approach still entails the process of measuring individual otoliths. Furthermore, otoliths are commonly broken during extraction and transportation which can heavily bias the morphometric information.

Fourier transform near-infrared (FT-NIR) spectroscopy is an emerging technology in fisheries and conservation biology (Helser et al., 2019a, 2019b; Vance et al., 2016; Wedding et al., 2014) which may offer an alternative to both morphometric and shape analyses. The technique relies on light from the near infrared region (12,800 – 4000 cm^{-1} wavenumbers) of the electromagnetic spectrum and absorbance patterns that reflect a sample's organic chemical composition. These spectra can then be compared among samples typically using multivariate statistical analysis and has the power to discriminate known variables (e.g., age, stock, or species) of interest when those variables affect spectral signatures of analyzed samples (Murray and Williams, 1987). FT-NIR spectroscopy has recently gained attention with its ability to predict fish age from otoliths (Wedding et al., 2014; Helser et al., 2019a, 2019b; Passerotti et al., 2020), as well as the potential to discriminate geographical differences within a species (Wedding et al., 2014; Benson et al., 2020). FT-NIR spectroscopy, if effective in distinguishing cryptic *Etelis* species, would provide a time efficient alternative to manual morphometrics using calipers or image analysis, especially of species with fragile otoliths prone to breaking, and could be used to differentiate future cryptic species from archived collections. Since FT-NIR spectroscopy scanning does not damage the sample (i.e., otoliths are scanned whole), otoliths may later be used for traditional fish ageing following spectral scans and the determination of species. Furthermore, the same FT-NIR spectra used to identify a species could be used to predict the age of that individual fish.

Herein, we examine the utility of two different methods to distinguish between archived otoliths of cryptic species *E. carbunculus* and *E. boweni*. We assessed the efficacy of both approaches using voucher otoliths from the Southwest (SW) Pacific Ocean which were previously identified to species using phenotypic and genetic differences. First, we followed a morphometric approach where we used principal component and discriminant analyses to differentiate between the two species, similar to methods developed and demonstrated by Wakefield et al. (2014). Secondly, FT-NIR spectroscopy was used to determine whether spectral signatures of otoliths could be discriminated by species. Following calibration and validation of voucher (i.e., known) data, we applied optimal models from each approach to predict and classify archived *Etelis* sp. (i.e., unknown species) otoliths previously collected around Guam, where *E. boweni* has not yet been documented (Andrews et al., 2021). The pros and cons of each classification method in terms of accuracy and efficiency are discussed in the context of providing reliable data for sustainable fisheries management.

2. Methods

2.1. Samples

Voucher otoliths from *E. carbunculus* and *E. boweni* were located at the Pacific Community Marine Specimen Bank archive based in New Caledonia (Smith et al., 2017). Fish were collected over two years between July 2012 and April 2014 from research surveys and commercial fishers who fished near seamounts and island reef slopes in the Exclusive Economic Zones (EEZs) of New Caledonia, Fiji, Tonga, and Vanuatu (range: −15.1–24.4° S, 164.9° E – 174.3° W) in the SW Pacific. Samples ($n = 93$) were chosen by fork length (FL) to capture the full size range of each species, as well as to maximize the overlap in their size distributions. Samples were selected to also minimize spatial variability, selecting samples as evenly from as few regions as possible (i.e., similar numbers of each species for each EEZ). Voucher *Etelis* samples were distinguished phenotypically at the time of capture based on the presence (*E. boweni*) or absence (*E. carbunculus*) of a black margin on the upper lobe of the caudal fin and a rounded (*E. boweni*) or acutely sharp (*E. carbunculus*) opercular spine (Andrews et al., 2016). Fork length was measured to the nearest 1 mm, wet weight was recorded to the nearest 0.1 g, and the sagittal otoliths were removed, rinsed, and stored dry.

Presumed *E. carbunculus* otoliths were collected from the waters around Guam (13.4° N, 144.7° E) at the Guam Fishermen's Cooperative from 2009–2019 ($n = 91$) and were archived at the Pacific Islands Fisheries Science Center in Honolulu, Hawai'i. Currently, these samples comprise a potentially mixed collection of cryptic species, *E. carbunculus* and *E. boweni*. As above, fork length (FL) was measured to the nearest 1 mm, wet weight was recorded to the nearest 0.1 g, and the sagittal otoliths were removed, rinsed, and stored dry. Guam samples were not tested genetically at the time of capture, and no tissue remains with which to corroborate species identification.

2.2. Otolith morphometric measurements

The right otolith was selected as the target for morphometric analysis, as voucher samples only had right side otoliths available. Unfortunately, damage occasionally occurred for otoliths on either side during extraction or archival storage. When a whole right otolith was not available for a given sample, the left otolith was substituted (if unbroken). Measurements from right and left otoliths of the same individual

do not appreciably vary. Otolith measurements were taken using digital calipers (Brown & Sharpe IP40) and recorded to the nearest 0.01 mm. The terminology and methods of measurements used to describe the otolith shape follow those of Wakefield et al. (2014) and include 1) otolith length (i.e., length from rostrum to post rostrum), 2) otolith width (i.e., width from dorsal to ventral otolith edge at the widest point), and 3) otolith thickness (i.e., thickness from proximal to distal edge). All measurements were taken through (or across) the primordium.

Four additional morphometric measurements were made using imaging software (Image Pro, version 10.0) in the case that discrimination between species could not be made from caliper measurements alone. Area and perimeter were measured as they were expected to differ significantly between the two *Etelis* species; *E. boweni* is deeply lobed with rough margins in comparison to *E. carbunculus* (Andrews et al., 2021; Fig. 1). Length of the excisura major (i.e., distinct notch in otolith rim between rostrum and antirostrum) was measured as a proxy for otolith length because it would not be impacted by frequent rostrum breaks that impact the overall length metric. Sulcus groove width (i.e., sulcus acusticus) was measured based on prior evidence of morphological differences between the species (Andrews et al., 2021; Fig. 1).

Otolith images were captured by positioning the otolith microscope stage with their respective dorsal edge to the top of the image, anterior (rostral) region to the left and sulcus-side-up (proximal) (Fig. 1). A high resolution image of the right otolith from each individual was captured with a Zeiss Axiocam 506 color digital camera (Germany) fitted to a stereo binocular Zeiss AxioZoom V16 microscope (Germany) under appropriate magnification and using reflected light. Photographs were taken on a black background with scale bars under respective magnifications (Fig. 1). Image Pro analysis software (version 10.0) was used to acquire additional otolith morphometric measurements and to collect length and width from images to compare with values obtained using calipers. Metrics of otolith length, width, area, and perimeter were determined from otolith outlines. Length and width of each otolith was obtained from the maximum horizontal axis and maximum vertical axis of the smallest bounding rectangle around the otolith outline. Any cotton fibers or dried organic material that disrupted the otolith outline shape were manually removed or edited out of the outline images to remove bias. Measurements of excisura length and sulcus groove width over the primordium were measured using the line measure tool. Image-based measurements provide only a two-dimensional representation of otolith morphology and thus do not take into account otolith thickness or curvature.

To assess precision between measurement methods, the correlation between caliper-derived and image analysis-derived metrics of length and width were tested with Pearson's *r*. Some breaks occurred or worsened between measurements while in transit between laboratories as indicated by large (>1 mm) disparities, so these samples ($n = 6$) were excluded from analyses of precision between measurement methods.

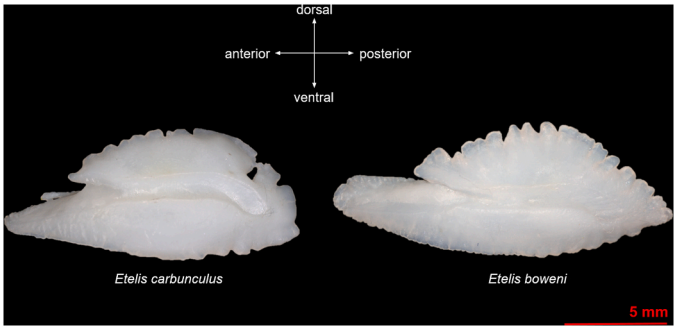

Fig. 1. Proximal view of right sagittal otoliths from *Etelis carbunculus* (50 cm FL, left), and *Etelis boweni* (67 cm FL, right). Scale bar (in red) is 5 mm.

2.3. Otolith morphometric discrimination

2.3.1. Whole versus broken otoliths

Considering the frequency of breaks among our samples plus the likelihood of frequent breaks in future collections, separate analyses were performed on whole (i.e., unbroken) otoliths, as well as all otoliths in the collection regardless of chips and breaks. Samples with at least one whole intact otolith (left or right) were measured for all otolith metrics including three (length, area, and perimeter) that are impacted by breaks in the rostrum otolith. Analyses that included all otoliths used the right otolith, when available, and included only four metrics (width, thickness, excisura major length, and sulcus groove width) which are not affected by rostrum chips and breaks.

2.3.2. Principal component analysis and ANOVA

Multivariate Principal Component Analysis (PCA) was performed on otolith morphometrics of voucher specimens to visually assess the degree of morphological difference between each species and identify which variables had the greatest variation using the package prcomp in R (R Development Core Team, 2014). PCAs were calculated separately on the subset of whole otoliths and on all otoliths for the metrics unaffected by chipped or broken rostrums. All morphometric measurements of otoliths were size-standardized (measurement divided by FL) before analysis to reduce the effect of allometric differences between individuals and species.

Boxplots and summary tables were constructed to evaluate whether significant differences in the morphometric values existed between species. In addition, relationships between fish size and otolith morphometric variables for each species were investigated by fitting linear regressions of each of the otolith morphometric variables against fish length (FL). Differences in the slopes of the resulting regressions were initially tested with ANCOVA using species as the independent variable and FL as the covariate. However, FL and species were not independent, given inherent differences in maximum body size (Williams et al., 2015). Thus, one way ANOVAs were used to test for differences in otolith morphometrics standardized by fish FL between species.

2.3.3. Multivariate classification

Quadratic discriminant analysis (qda) was performed with the MASS package in R (R Core Team 2014) to generate combinations of otolith morphometric variables that maximize the probability of correctly assigned voucher samples to their species group (Quinn and Keough, 2002). As opposed to linear discriminant analysis, qda is useful when equal covariance matrices among classes (i.e., species) cannot be assumed. Only variables that were significantly different between species in ANOVAs were used in qda model building. Otolith morphometric variables were standardized by FL to account for differences in fish size prior to analysis. Leave-one-out-cross-validation was used to test the accuracy of species classifications based on known species membership of the voucher dataset. Essentially, one individual at a time was omitted from the dataset, the discriminant function was recalculated, and then the omitted individual was assigned to a group using the new function (Lachenbruch and Mickey, 1968). Klecka's tau (τ), a chance-corrected measure of accuracy accounting for potential biases arising from unequal group sizes, was also calculated (Klecka, 1980; White and Rutenberg, 2007). The predict function was used to assign class probabilities to all samples in the voucher dataset.

The simplest model with the highest discrimination (classification accuracy) was selected to maximize the robustness of the model when applied to new data. Models were then used to make predictions on the test *Etelis* sp. dataset from Guam. The voucher dataset was used to train the qda models, and the predict function was used to assign class probabilities to the test (i.e., Guam) dataset with no species classified prior. Predictions were made in the form of posterior probabilities (i.e., the probability that the observation belongs to the k^{th} class) which were plotted from each model to visualize species predictions.

2.4. FT-NIR spectroscopy

2.4.1. Spectral measurements and pre-processing

All otoliths were scanned proximal side down using diffuse reflectance on a Bruker Multi Purpose Analyzer II Fourier transform Near Infrared Spectrometer with a 22-mm diameter sample window and OPUS software (version 7.8; Bruker Scientific, Billerica, MA). The spectrum acquisition was performed from 10,000 cm^{-1} to 4000 cm^{-1} (64 scans, resolution 16 cm^{-1}). Scans were averaged to produce a single representative spectrum for each sample.

Following acquisition, spectral data were uploaded into Solo 8.9.2 (2021), a chemometric software that uses a MatLab framework (Eigenvector Research Inc., Manson, WA) for data processing and model generation. Selected spectral regions were in the 7500 to 4000 cm^{-1} range. Raw spectra were plotted to detect any outliers in need of rescanning. Spectral data were pre-processed with 13-point Savitzky-Golay smoothing (2nd order polynomial), 13-point Savitzky-Golay first derivative transformation, and mean-centering which produced the best separation among groups.

2.4.2. Principal component analysis

Exploratory data analysis based on PCA was performed to visualize trends in the voucher data and to evaluate the discriminatory possibility of the FT-NIR spectra between species. PCA on the pre-processed data matrix was obtained using two or three principal components, and cross-validation (CV) was performed using Venetian blinds with ten splits (10 sub-validation sets of 8 samples each) and algorithm-SVD (Singular Value Decomposition). Species groups were visualized using a scores plot. Hotelling's T^2 and Q residuals were inspected to detect any spectral outliers in need of rescanning.

2.4.3. Multivariate classification

Partial least squares discriminant analysis (PLS-DA) was used to evaluate spectral variability from voucher *E. carbunculus* and *E. boweni* based on a known class membership (i.e., species) of the samples. To obtain the discrimination model, each *Etelis* species was defined as a separate class. PLS-DA models on voucher data were calibrated and validated using two approaches. First, the entire dataset was used to calibrate a discrimination model, and CV of the model was executed using Venetian blinds with ten splits. For the second approach, the total sample set was partitioned into: calibration (assembled from 70% of samples), and validation datasets (the remaining 30% of samples). The split was done using the Kennard-Stone algorithm within Solo (Kennard and Stone, 1969). The calibration dataset was used to generate the classification model (Venetian blinds CV), and the validation dataset was used to evaluate predictive (i.e., classification) performance after assigning class membership to one of the two species.

In each case, automatic variable selection (in Solo) was used to find subsets of variables (i.e., wavenumber regions) that maximize model accuracy (compared to all 949 variables). Goodness of fit for each model was based on the cross-validation (CV) error, R^2 (coefficient of determination), RMSECV (root mean square error of cross validation), and specificity (true negative rate) and sensitivity (true positive rate) of the model. Class error was calculated for each model as the average of the false positive and false negative rates and was viewed as a confusion matrix.

Lastly, PLS-DA models built on voucher samples were used to predict class (i.e., species) membership of the Guam *Etelis* sp. samples. The PLS-DA classification method builds a model on the calibration dataset (e.g., voucher) and, by default, assumes the two classes have equal prior probability, regardless of the relative number of samples of each class in the calibration dataset. However, if there is known information on the prior probability of each class in the population, it is possible to incorporate these priors into the model's classification so that the model would be more accurate for datasets randomly sampled from that population. The assumption that classes were evenly distributed in Guam samples was not met based on evidence of far more *E. carbunculus* (~80%) compared to *E. boweni* (~20%) in the dataset; thus, prior probabilities of the PLS-DA model were modified using "priorprob." Species predictions of these samples were compared to qda results from otolith morphometrics.

3. Results

Despite outward similarities in phenotype, *E. carbunculus* reaches a much smaller maximum size compared to *E. boweni*. Fork length (FL) of voucher samples ranged from 25.0 to 58.0 cm for *E. carbunculus* ($n = 38$) and from 29.0 to 85.0 cm for *E. boweni* ($n = 45$) (Pacific Islands Fisheries Science Center, 2020) (Fig. 2, Table 1). Mean (± SE) FL was 42.26 (± 1.49) cm for *E. carbunculus* and 53.47 (± 2.43) cm for *E. boweni* (Fig. 2, Table 1). Out of all 83 voucher samples, only 22% ($n = 18$) had whole, unchipped otoliths for morphometric measurements. The remaining otoliths ($n = 65$) had material missing from the right otoliths from chipped or completely broken rostrums. Fork length of Guam samples ranged from 18.1 to 89.0 cm (Fig. 2, Table 1). Out of all 91 Guam samples, only 20% ($n = 19$) had otoliths pairs in whole condition for morphometric measurements (i.e., no rostrum breaks), whereas 24 samples had a whole right ($n = 15$) or left ($n = 9$) otolith. The remaining 48 samples (>50%) had material missing from both right and left otoliths from chips or breaks.

3.1. Otolith morphometrics

3.1.1. Precision: Caliper versus image measurements

Length metrics were nearly identical between caliper and image measurements. There was a strong positive correlation ($p < 0.001$; $r = 0.99$) between caliper-derived length and image analysis-derived length metrics (Fig. S1). The linear regression between length metrics was significant ($p < 0.001$), and there was nearly a 1:1 agreement between methods used to obtain them (Fig. S1). There was also a strong positive correlation ($p < 0.001$; $r = 0.99$) between caliper-derived width and image analysis-derived width metrics (Fig. 3). The linear regression between width metrics was significant ($p < 0.001$), though less agreement is apparent between methods (Fig. S1). This is likely due to the caliper-derived width being taken through the otolith

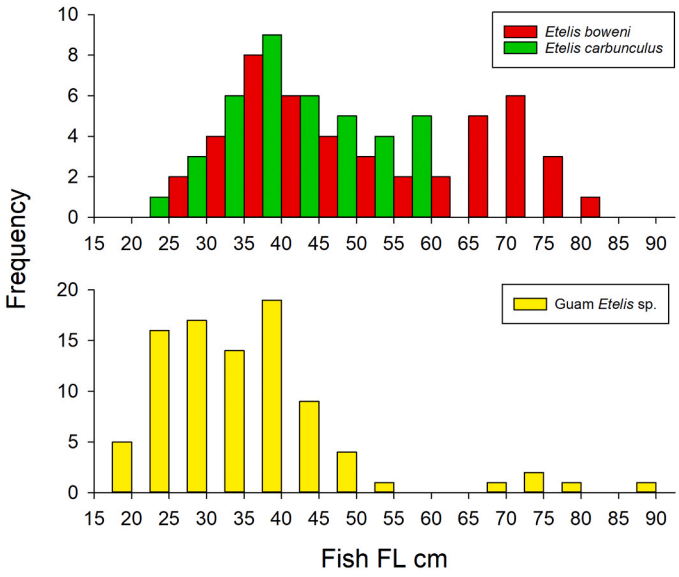

Fig. 2. Length frequency distribution of voucher *Etelis carbunculus* (green, $n = 39$) and *Etelis boweni* (red, $n = 46$) specimens from the SW Pacific, and *Etelis* sp. ($n = 91$) previously collected from the Guam bottomfish fishery, which were assumed to be all *E. carbunculus* but are now known to be a mix of the two species.

Table 1
Descriptive statistics for fish fork length, fish weight, and seven otolith morphometric variables for voucher *Etelis carbunculus* and *Etelis boweni* from the SW Pacific and for *Etelis* sp. from Guam. Sample sizes (*n*) differ by variable depending on whether whole (i.e., unbroken) otoliths (*) were used or whether field data existed for the sample. Morphometric abbreviations are noted in parentheses.

	SW Pacific voucher samples									Guam samples				
	Etelis carbunculus					*Etelis boweni*				*Etelis* sp.				
Metrics	Range	Mean	SE	*n*		Range	Mean	SE	*n*	Range	Mean	SE	*n*	
Fork length, cm	25.0 – 58.0	42.26	1.49	38		29.0 – 85.0	53.47	2.43	45	18.1 – 89.0	34.77	1.44	91	
Fish weight, kg	0.28 – 3.70	1.59	0.17	38		0.40 – 11.10	3.79	0.47	43	0.10 – 13.32	1.11	0.21	90	
Otolith length, mm (L)	10.6 – 14.4	11.80	0.48	8	*	11.6 – 17.4	15.35	0.67	10	*	7.7 – 20.6	10.89	0.38	43	*
Otolith width, mm (W)	4.69 – 8.85	6.25	0.16	38		3.88 – 7.61	5.84	0.14	45	3.5 – 8.2	5.13	0.11	91	
Otolith thickness, mm (T)	1.17 – 2.65	1.78	0.06	38		0.99 – 2.16	1.37	0.04	45	0.88 – 3.04	1.33	0.04	91	
Otolith area, mm^2 (A)	39.0 – 72.5	49.32	4.50	8	*	40.0 – 72.4	60.72	3.70	10	*	19.2 – 85.5	38.76	2.24	43	*
Otolith perimeter, mm (P)	30.2 – 48.7	36.35	2.40	8	*	33.6 – 72.4	43.74	2.10	10	*	20.7 – 60.2	31.09	1.23	43	*
Otolith sulcus groove width, mm (S)	0.78 – 1.28	1.04	0.02	38		0.59 – 1.17	0.85	0.02	45	0.58 – 1.39	0.90	0.02	91	
Otolith excisura major length, mm (E)	6.84 – 9.63	8.26	0.12	36		7.18 – 13.93	10.25	0.29	40	5.3 – 12.2	7.67	0.15	91	

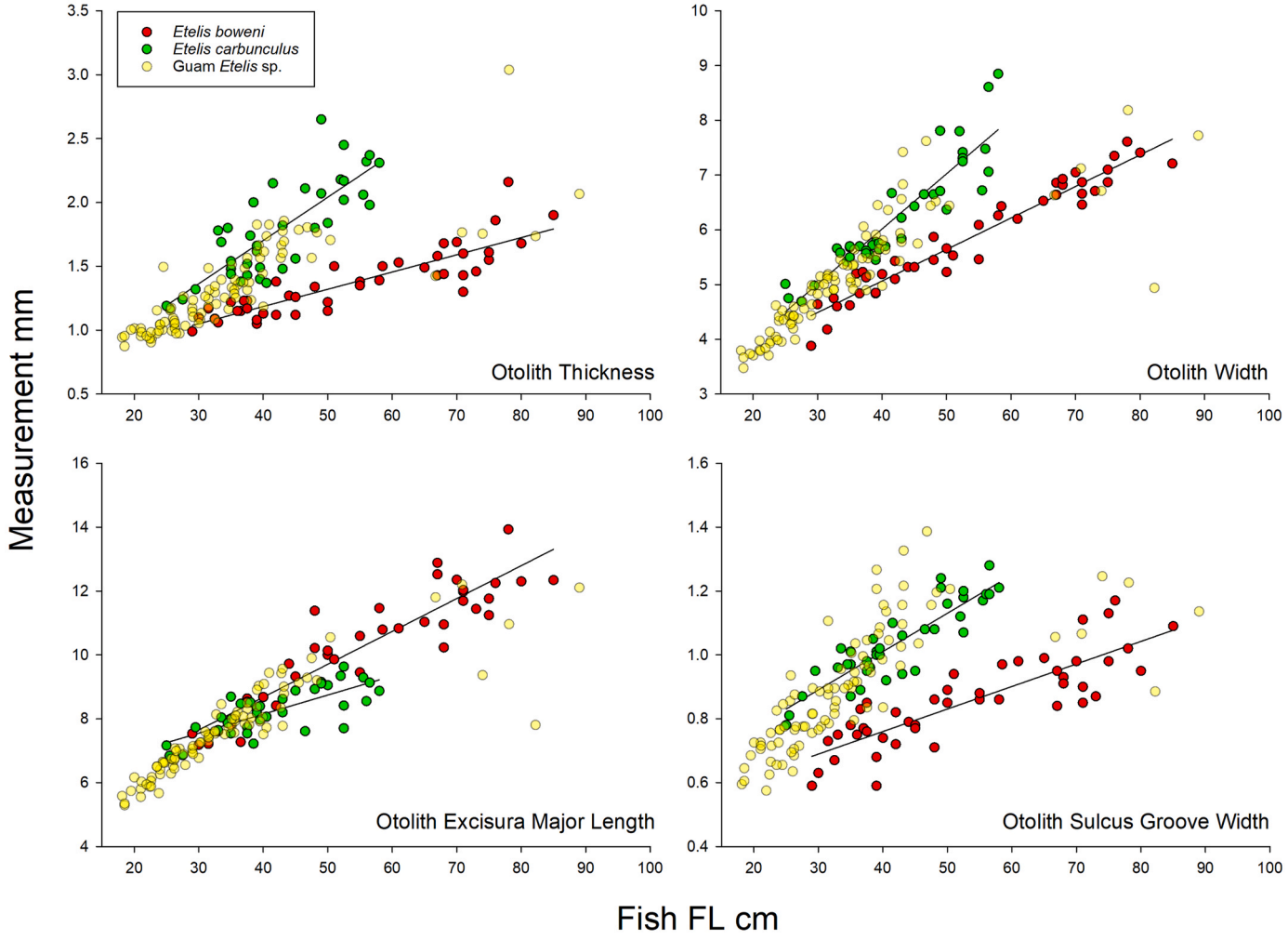

Fig. 3. Relationships between otolith thickness, width, excisura major length, and sulcus groove width corresponding to fork length of voucher *Etelis carbunculus* (green) and *Etelis boweni* (red) from the SW Pacific. *Etelis* sp. from Guam are overlaid in yellow. All voucher ($n = 83$) and Guam ($n = 91$) otoliths were plotted regardless of rostrum breaks, as thickness, width, excisura length and sulcus groove width metrics should be unaffected.

primordium, whereas the bounding rectangle used to measure the widest point of the otolith in image analysis may not always correspond to the width at the primordium. Measurements of otolith length and width from Image Pro were used in downstream analyses, given the high correlation between caliper and digital measurements.

3.1.2. Otolith morphometric discrimination

The PCA on whole (i.e., intact) voucher otoliths ($n = 18$) showed grouping between species, with perfect separation provided by inclusion of all seven morphometric variables (Fig. S2A). Most of the variation in the multivariate morphometric data (96.2%) was described by PC1 (73.5%) and PC2 (16.8%) and PC3 (5.9%) (Table S1). PC loadings indicated that otolith width, perimeter, thickness, and sulcus groove

width had the largest contribution to PC1, whereas otolith excisura major length and overall length had the largest contribution to PC2 (Table S1, Fig. S2A).

The PCA on all voucher otoliths ($n = 74$) also showed significant grouping between species, with near-perfect separation provided only the morphometric variables that were not impacted by chips and breaks were used (Fig. S2B). Most of the variation in the multivariate morphometric data (97.2%) was described by PC1 (82.7%) and PC2 (14.5%) (Table S1). PC loadings indicated that otolith width, sulcus groove width, and thickness had the largest contribution to PC1, whereas otolith excisura major length had the largest contribution to PC2 (Table S1, Fig. S2A).

Relationships between FL and various morphometric measurements of voucher otoliths revealed some clear distinctions between species (Fig. 3). Compared to *E. boweni*, *E. carbunculus* have relatively thick, wide otoliths with deep sulcus grooves (Fig. 3). The relationship between FL and otolith length was highly overlapping between species, besides *E. boweni* reaching a much larger maximum size (Fig. S3). Relationships between FL and otolith morphometrics of area and perimeter provided less separation between species, but suffered from low sample size of whole, intact otoliths (Fig. S3). Compared to *E. boweni*, *E. carbunculus* have otoliths with relatively large area and perimeter (Fig. 3). ANOVA revealed that, out of the seven otolith morphometric measurements examined, there were significant differences between species means of five measurements – thickness, width, sulcus groove width, perimeter, and length (Fig. 4). The greatest differences between species were observed for thickness ($p < 0.001$), width ($p < 0.001$), and sulcus groove width ($p < 0.001$) (Fig. 4) which corroborated PCA results.

Guam *Etelis* sp. samples were overlaid on species-specific relationships, and the largest individuals (≥60 cm FL) broadly grouped with *E. boweni* voucher samples (Fig. 3). However, two large *Etelis* sp. from Guam departed from general patterns of voucher *E. boweni*, with one (78 cm FL) having a relatively thick otolith more similar to *E. carbunculus*, and one (82 cm FL) having a relatively narrower otolith than either species. Due to a high amount of overlap at smaller FLs, otolith morphometric variables could not easily single out potential *E. boweni* < 60 cm FL in the archived collection of samples from Guam (Fig. 3).

Depending on the classification dataset (i.e., whole only versus all otoliths), maximum accuracies of qda models trained and cross-validated using voucher data ranged between 92.8% and 100% (chance-corrected CA: 85.5–100%) (Table 2). When fit with only whole otoliths, eight different model combinations resulted in 100% classification accuracy (chance-corrected CA: 100%) (Table 2). The simplest of these models used only otolith width and thickness as variables to

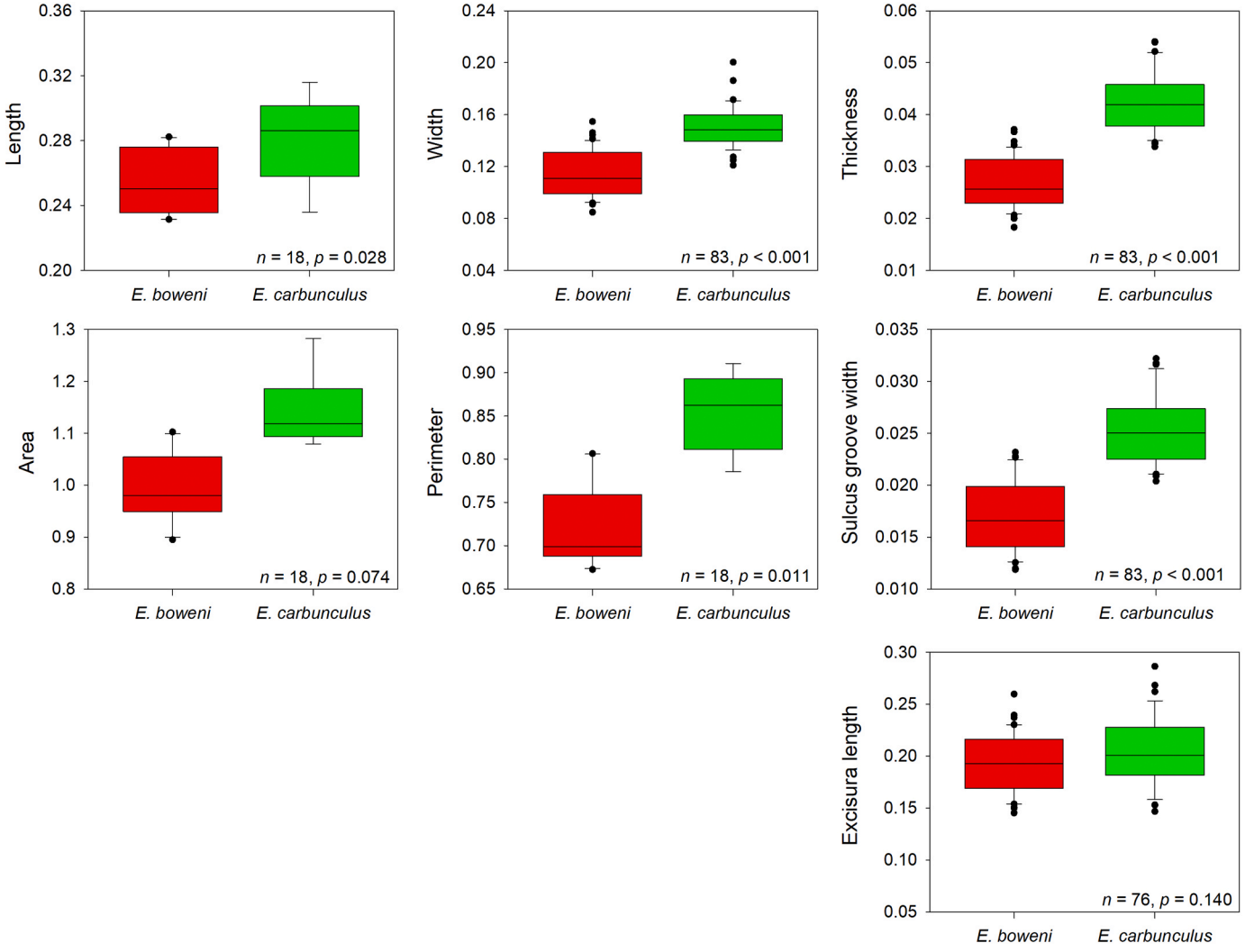

Fig. 4. Boxplots displaying the differences between seven otolith morphometric variables of voucher *Etelis carbunculus* (green) and *Etelis boweni* (red) from the SW Pacific. Plots display relative measurements which were standardized by fork length, not raw measurements. Units for each morphometric variable are the same as those found in Table 1. Sample sizes are indicated in each panel, along with *p*-values from ANOVA.

Table 2
Cross-validation (leave-one-out) classification accuracy (CA) estimated from quadratic discriminant analysis models of otolith morphometric variables on the voucher samples from the SW Pacific. All morphometric variables were standardized by fish size (FL). All morphometric variables were included when classifying whole otoliths, and only width, thickness, and sulcus groove width were included when classifying the entire dataset, which included otoliths with chips and breaks. Chance-corrected CA was estimated using Klecka's Tau (Klecka, 1980; White and Ruttenberg, 2007).

Dataset	Model: Species ~	No. of Variables	Classification Accuracy (%)	Chance-corrected CA (%)
All otoliths ($n = 83$)	Width + Thickness + Sulcus	3	92.8	85.5
	Thickness + Sulcus	2	92.8	85.5
	Thickness	1	92.8	85.5
	Width + Thickness	2	91.6	83.1
	Sulcus	1	86.7	73.5
	Width	1	85.5	71.1
	Width + Sulcus	2	84.3	68.7
Whole otoliths only ($n = 18$)	Width + Thickness + Sulcus + Length	4	100	100
	Width + Thickness + Sulcus + Perimeter	4	100	100
	Width + Thickness + Length + Perimeter	4	100	100
	Width + Thickness + Sulcus	3	100	100
	Width + Thickness + Length	3	100	100
	Width + Thickness + Perimeter	3	100	100
	Width + Sulcus + Length	3	100	100
	Width + Thickness	2	100	100

predict species. When fit instead with all otoliths, the model using variables of thickness, width, and sulcus groove width provided the highest classification accuracy (92.8%, chance-corrected CA: 85.5%); however, thickness and sulcus groove width as well as thickness alone provided the same predictive ability for the voucher data (Table 2). The qda models on all otoliths predicted 95.6% of *E. boweni* species correctly, misclassifying only three as *E. carbunculus*, and predicted 92.1% of *E. carbunculus* species correctly, misclassifying only two as *E. boweni*. The size range of the misclassified voucher samples was 31.5 to 45 cm FL.

Considering the high proportion of chipped and broken otoliths from Guam, the two best models fit using all (instead of whole) otoliths were used to make predictions on unknown Guam *Etelis* sp. samples. When thickness, width, and sulcus groove width were included, the model predicted that all samples were *E. carbunculus*, except for seven which it classified as *E. boweni* (Fig. 5A). The model predicted that the largest samples (≥60 cm FL) were all *E. boweni* except one (GVDP-0370). Two samples (GGBS-0064, GECC-1690) classified as *E. boweni* by this model were within the size range of both species (35.5 and 40 cm FL, respectively) (Fig. 5A). When only width and sulcus groove width were included, the model predicted that all samples were *E. carbunculus* except seven samples which were classified as *E. boweni*, which differed slightly from the predicted sample set above (Fig. 5B). In this case, the model predicted that all of the largest samples (≥60 cm FL) and only one sample (GGBS-0064) smaller than 60 cm were *E. boweni*. Overall, both morphometric models predicted that only 8% (7 of 91) of archived otoliths belonged to the newly identified *E. boweni*.

3.2. FT-NIRS

3.2.1. FT-NIRS Spectra

Spectral data from the *Etelis* otoliths showed distinct absorbance patterns (i.e., peaks and valleys at certain wavenumbers) typical of other fish otoliths (Fig. S4). A total of 12 samples in the voucher dataset and one sample in the Guam dataset were rescanned due to abnormally high peaks apparent in spectral absorbance, and the best spectra was selected for analysis. Distinct peaks among all spectra were observed at approximately 6800 cm^{-1}, 5160 cm^{-1}, and 4300 cm^{-1} (Fig. S4). When voucher spectral data were pre-processed, species separation became apparent in several wavenumber regions, with the largest differences observed around 7100 cm^{-1}, 5300 cm^{-1}, 4400 cm^{-1}, and 4000 cm^{-1} (Fig. 6).

3.2.2. Principal component analysis

The PCA on pre-processed voucher data included all 949 wavenumber regions as variables and showed significant clustering between species (Fig. 7), thus demonstrating the possibility of classifying *Etelis* sp. samples based solely on FT-NIR spectral signatures. Most of the variation in the multivariate morphometric data (99.4%) was described by PC1 (96.96%) and PC2 (2.48%) (Fig. 7). The two species clusters were clearly separated along PC1 and PC2 despite some overlap.

3.2.3. Multivariate classification with PLS-DA

A total of 46 *E. boweni* and 39 *E. carbunculus* voucher sample spectra were used to calibrate PLS-DA models. Variable selection for each model identified 480 (fully cross-validated) and 623 (test split) wavenumber variables (out of 949) as the most important for discrimination between spectra. The fully cross-validated PLS-DA model was computed with 4 latent variables (LVs) and performed nearly perfectly for species classification, with a class error rate of 2.4%. The model correctly classified 83 voucher samples into *E. boweni* ($n = 45$) and *E. carbunculus* ($n = 38$) classes (Table 3, Fig. S5). Only one sample of each species was misclassified in cross-validation. Both specificity (0.974) and sensitivity (0.978) were very high.

Comparable results were observed when voucher samples were split into calibration (70%, $n = 60$) and external validation (30%, $n = 25$) datasets (Table 3, Fig. S5). Class error of the calibration CV was 5.0%, and only one *E. boweni* and two *E. carbunculus* were misclassified (Table 3). The PLS-DA model also performed very well for true predictions on the external validation dataset and correctly predicted the species class of 24 voucher samples without information on the true species. Only one *E. carbunculus* was misclassified as *E. boweni* (Table 3, Fig. S5). The class error for the validation set was slightly lower than the calibration at 4.0%.

The fully cross-validated model (lowest class error rate) was used to test predictions on the archived Guam *Etelis* sp. samples. Prior probabilities were modified so that the model would not assume an equal probability of observing either species, as *E. boweni* appear to be rare in Guam (an assumption which was corroborated by morphometric results herein). The model predicted that 8% (7 of 91) of archived otoliths belonged to the newly identified *E. boweni*. Two Guam samples over 60 cm FL (GECC-1133, GECC-1317) were classified as *E. boweni* from predictions made on voucher-calibrated PLS-DA model which we assume to be a correct species assignment (Fig. 8). Three Guam samples over 60 cm FL (GECC-0318, GVDP-0370, and GVDP-0503) were classified as *E. carbunculus* which we assume to be false, based on maximum reported FL of the species (Fig. 8). However, sample GVDP-0370 stood out as an outlier in the overall plot of Hotelling's T^2 and Q residuals, so

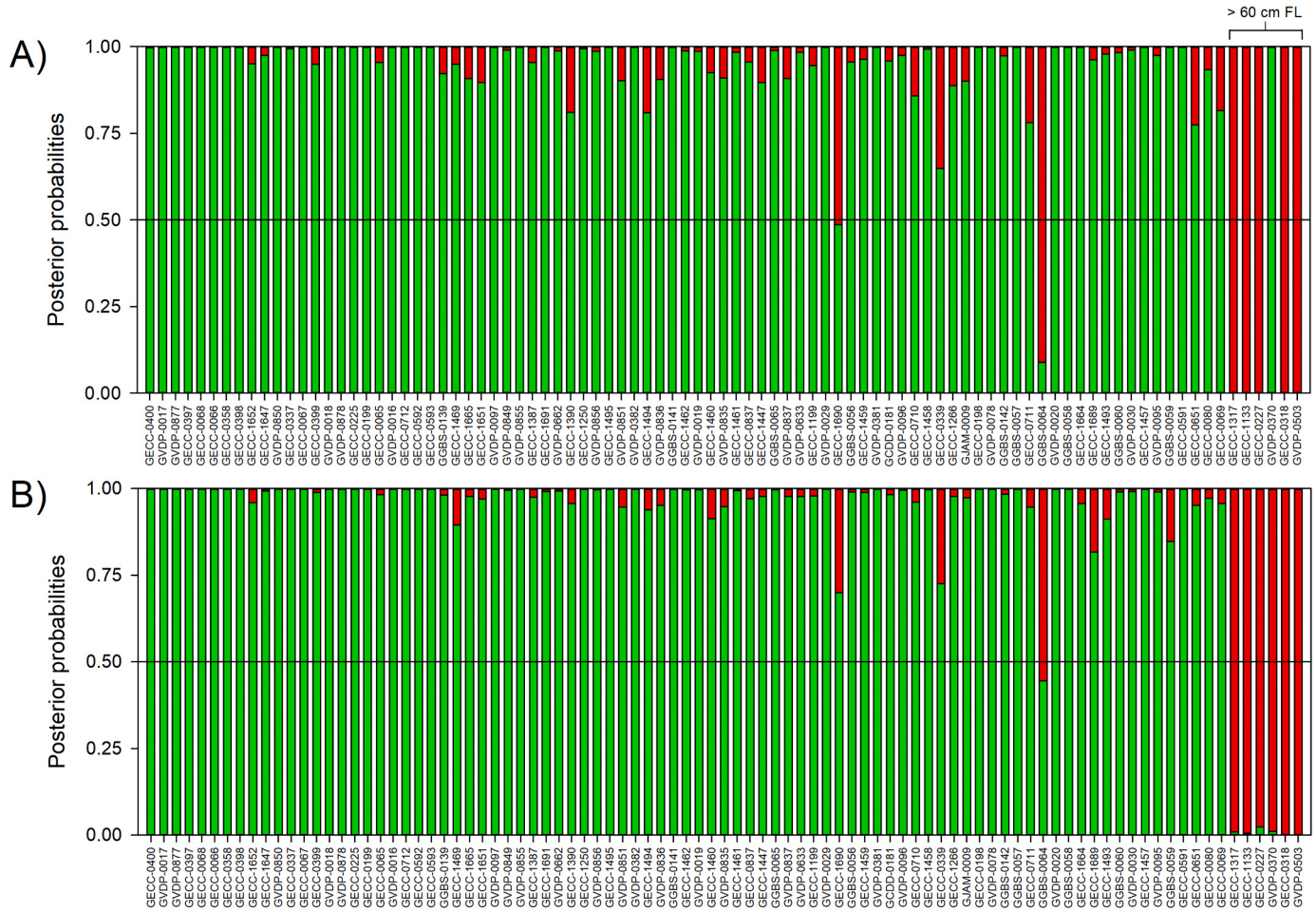

Fig. 5. QDA model predictions for Guam *Etelis* spp. ($n = 91$) into *Etelis carbunculus* (green) and *Etelis boweni* (red) classes, based on morphometric data for otolith A) width, thickness, and sulcus groove width and B) width and sulcus groove width only. Samples are sorted on the x-axis from smallest FL to largest FL (left to right), with the largest individuals over 60 cm indicated. A reference line at 0.5 probability is drawn, along which class predictions were made.

prediction on this sample is unresolved. Five additional Guam samples were classified as *E. boweni*: GECC-0069 (50.4 cm), GECC-0591 (46.8 cm), GECC-0711 (39.9 cm), GECC-1494 (30.4 cm), and GVDP-0381 (35.7 cm) (Fig. 8). Two individuals (GECC-1133, GECC-1317) were identified as *E. boweni* by both methods, lending more credibility to their species identity.

4. Discussion

Differentiation of the cryptic species pair *Etelis carbunculus* and *Etelis boweni* was shown to be possible and highly reliable through examination of archived otoliths. Significant and distinguishable differences in otolith morphometrics were observed between *E. carbunculus* and *E. boweni* voucher samples collected in the SW Pacific. This study also explored the use of Fourier transform near-infrared (FT-NIR) spectroscopy as a potential new method to distinguish the cryptic species pair. FT-NIR spectral absorbance patterns of archived voucher otoliths from the SW Pacific were distinct between species. Classification models applied using both morphometric measurements and NIR spectral data were able to predict species with a high degree of accuracy despite a relatively large spatial area of voucher specimen collection ($\pm 10^{\circ}$ latitude and longitude) and regardless of whether otoliths were whole (i.e., unbroken). In addition, each method indicated the presence of the newly described *E. boweni* species in the archived collection of *E. carbunculus* otoliths captured around Guam. Though species identification could not be corroborated with genetic (or other) methods, results presented here provide strong evidence that the species' distributions overlap in this region. The purported identification of both *E. carbunculus and E. boweni* in the archived catch from Guam has important implications for fisheries management; therefore, it is imperative that the corresponding otolith collections are examined to ensure that the otoliths are assigned to the correct species.

It is well understood that otolith shapes differ between teleost species (Gaemers, 1984) including, to a lesser degree, closely related and cryptic species (Bani et al., 2013; Wakefield et al., 2014; Zischke et al., 2016; Moore et al., 2022). Though voucher *Etelis* otoliths appeared very similar, simple morphometric measurements captured key differences in shape in this cryptic species pair. For a given fish length, otoliths of *E. boweni* were slender, with a distinctly elongate and pointed rostrum (when unbroken), deeply crenulated margins, and a relatively narrow sulcus groove compared to *E. carbunculus*.

Basic caliper-derived otolith measurements as opposed to more complicated shapes have been previously used to discriminate *E. carbunculus* and *E. boweni* collected in the Indian and SW Pacific Oceans with high accuracy (>90%) (Wakefield et al., 2014). It was expected that morphometrics would be able to distinguish more recent samples from the same region; however, a high prevalence (>55%) of rostrum chips and breaks in the archived otolith collections of both SW Pacific voucher and Guam *Etelis* sp. prevented the usage of certain metrics for predicting species (e.g., length, area, perimeter). Our inclusion of additional measurements unaffected by breaks served to strengthen the discriminatory power of qda models which were highly

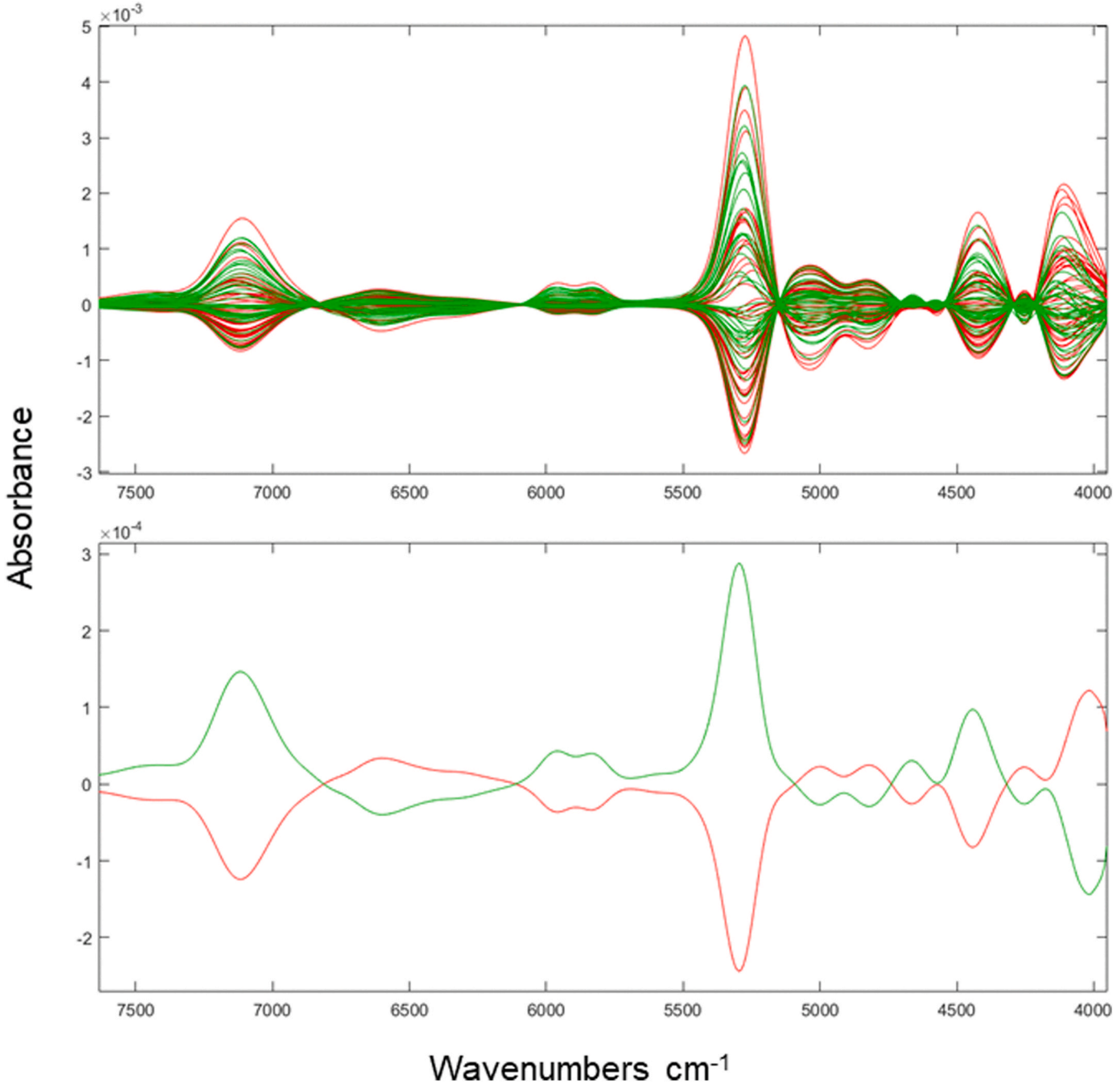

Fig. 6. Raw (top) and average (bottom) FT-NIR spectra (10,000 – 4000 cm^{-1}) of voucher *Etelis carbunculus* (green) and *Etelis boweni* (red) otoliths by species ($n = 85$), pre-processed by 13-point Savitzky-Golay smoothing (2nd order polynomial), 13-point Savitzky-Golay first derivative transformation, and mean-centering.

accurate (>90%) at predicting cryptic *Etelis* species, regardless of whether otoliths were whole. Classification models performed perfectly (100% accuracy) on whole, unbroken otoliths, where the simplest model included only width and thickness as predictor variables. When considering all otoliths, qda models were able to discriminate species with high accuracy (~93%) using only width, thickness, and sulcus groove width. Notably, simpler models using thickness and sulcus groove width, and even thickness alone, performed equally well. Otolith thickness relative to fish body length is a metric unaffected by breaks that occur frequently on delicate rostrums and will be useful to other archived collections. In addition, thickness can be measured from archived thin sections of previously aged fish potentially allowing for species discrimination of individuals without a matching whole otolith.

FT-NIR spectroscopy was also able to identify and separate the two cryptic *Etelis* species in this study with extremely high classification accuracy. The model performed best when making predictions for voucher data, indicating spatial (or some other) variability existed within both *Etelis* species from these distant sampling locales. Further, while exploring the spectral data, we observed PCA clustering of fish based on region within voucher samples. Thus, FT-NIR spectroscopy may be a useful tool to also discriminate spatial differences (e.g., stock discrimination) in these species and conceivably others. Robins et al. (2015) also reported evidence of spatial discrimination using this method. The best solution to avoid such geographic issues is to include samples from all locations in the calibration stage, in which case, the full scope of otolith microchemistry variation that may be encountered in

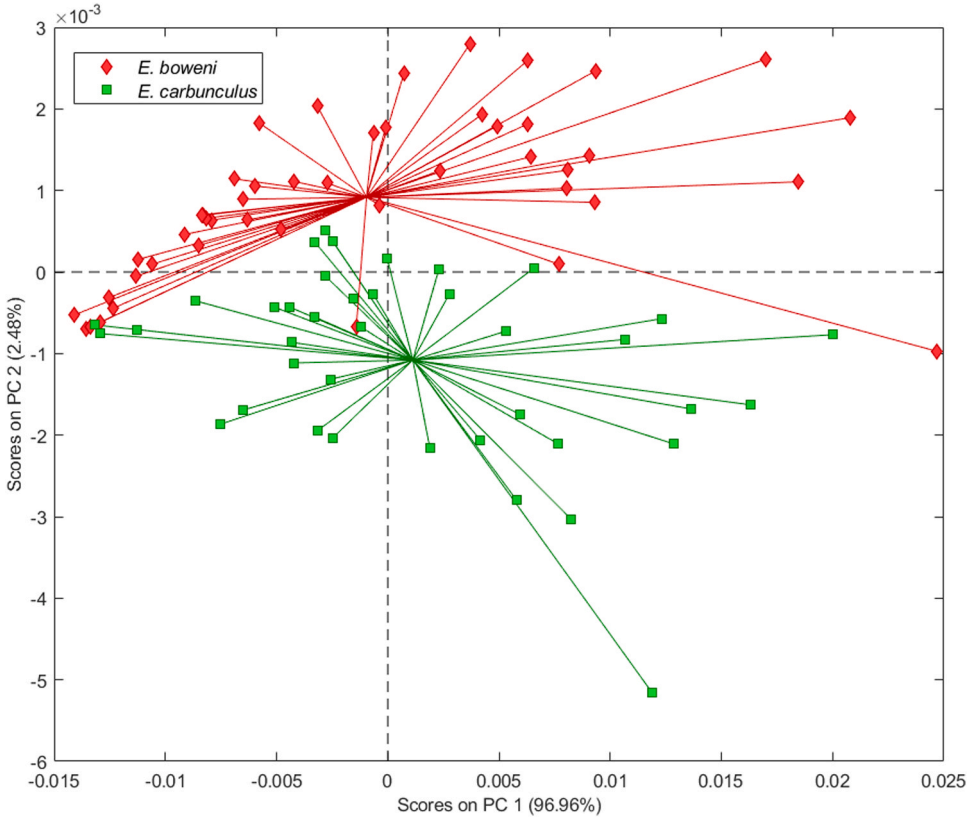

Fig. 7. Scores plot of PC1 and PC2 from PCA of FT-NIR spectral data from voucher otolith samples colored by species.

Table 3
Confusion tables for cross-validation and external validation of PLS-DA models on spectral data obtained via FT-NIR spectroscopy fit using voucher samples from the SW Pacific. Samples in bold are the correct species assignments based on known species of the voucher dataset.

				Actual Class	
Dataset	Model	*n*	Predicted as	*E. boweni*	*E. carbunculus*
Full cross-validation	Calibration	85	*E. boweni*	**45**	1
			E. carbunculus	1	**38**
Split-Test	Calibration	60	*E. boweni*	**32**	1
			E. carbunculus	2	**25**
	Validation	25	*E. boweni*	**12**	1
			E. carbunculus	0	**12**

the test dataset is captured by the model (Robins et al., 2015). Had our calibration models included some spectra from fish collected in Guam (for which species identification could be confirmed), it would have undoubtedly improved predictions.

Species predictions from best models of each method suggested that archived otoliths from Guam belong primarily to *E. carbunculus* (92%: 84 of 91). In each instance, seven archived otoliths were predicted to belong to the newly identified *E. boweni*; however, each method predicted different individuals falling into each species group. Regardless of method, there was a general lack of overlap in body sizes between the two *Etelis* species identified in Guam. Based on morphometrics, samples that were apparent *E. boweni* included five individuals greater than 60 cm FL and two smaller individuals (35.5 and 40 cm FL). Based on FT-NIR spectroscopy, samples classified as *E. boweni* included two of the largest individuals (> 60 cm FL) and two smaller individuals (30.4 and 35.7 cm FL). Given what we know about maximum body sizes in *E. carbunculus* (<60 cm FL), it appears that otolith morphometrics provided more reliable predictions of these cryptic species. However, when interpreting these results, it is important to note that fish length was not incorporated in the FT-NIR spectral analysis, while morphometrics were scaled with fish length. Furthermore, FT-NIR spectral data may be linked to, or driven by physical (e.g., morphometric) differences in the otoliths themselves, in addition to the potential chemical differences among cryptic species otoliths.

Predictive models for both morphometrics and FT-NIR spectroscopy approaches are only as good as the calibration data provided for training models. An important assumption of these analyses is that each voucher specimen was correctly identified to species. Voucher specimens were collected after recognition of the new cryptic species and the identification of the distinguishing external characteristics. However, the presence of the dark margin on the upper lobe of *E. boweni* caudal fin is not always easy to see and the 'sharpness' of the opercular spine is relative between the two species and not always obvious. While we are not questioning the ability of the researchers to correctly identify the fish used in this study, the possibility of a misidentification cannot be discounted.

In summary, differentiation of voucher *Etelis carbunculus* and *Etelis boweni* specimens was shown to be possible and highly reliable through examination of otolith morphometrics as well as FT-NIR spectroscopy. With the widespread use of molecular genetic techniques, new cryptic species are regularly being identified in marine fishes, causing species identification issues and reexamination of past life history research. Preserved specimens are typically not available to resolve retroactive species classifications, but otoliths may be more readily available in life history archives. *Etelis carbunculus* and *Etelis boweni* exhibit certain external characteristics to separate modern samples, but this may not be possible of other cryptic species. Beyond this cryptic species pair, both methods may provide the same level of accuracy for other species and be applicable to archived otoliths when other cryptic species are identified subsequent to collection. Both methods have their pros and cons in terms of time and cost efficiencies. Case-specific, otolith morphometrics may

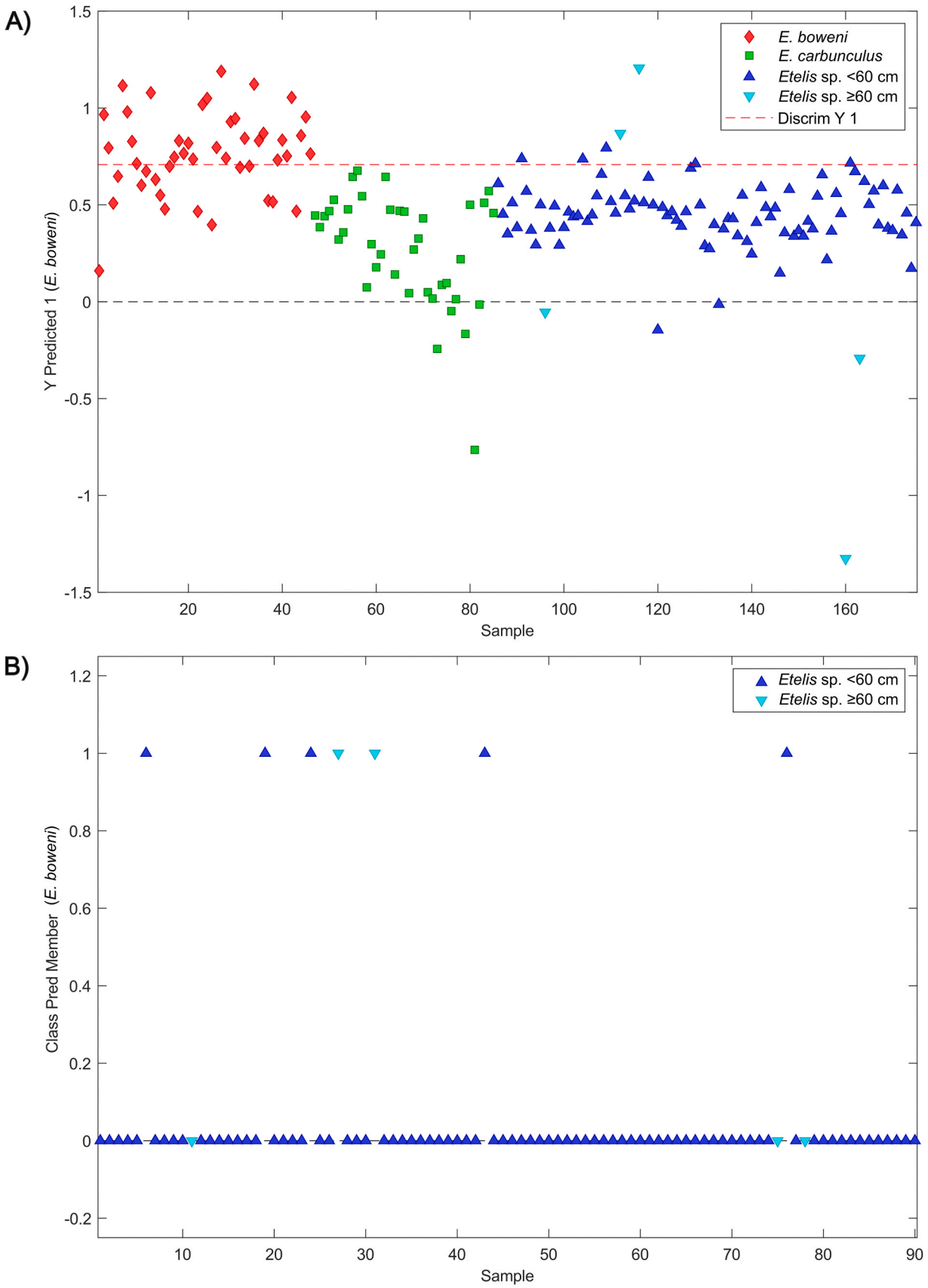

Fig. 8. PLS-DA model testing results showing the model trained on voucher FT-NIR spectra used to predict the species of Guam *Etelis* sp. samples. A) Samples 1–85 represent the calibration (i.e., training) dataset and samples 86–176 represent the Guam (i.e., unknown) dataset. The discrimination line (red dash) indicates the point at which samples above are predicted as *Etelis boweni* and below are predicted as *Etelis carbunculus*. Guam data are displayed by a size range cut-off, given that only *Etelis boweni* are expected to grow larger than 60 cm FL. B) Model predictions for *E. boweni* are shown.

be the preferred method if otolith length is not a distinguishing feature between the two species, otolith rostrums are not susceptible to breaking during extraction and transportation, and the archived sample size is not overwhelming; conversely, FT-NIR spectroscopy may provide greater accuracy and time efficiency. Finally, morphometric measurements are less expensive data to collect, and may be more conducive in cases where cost is a limiting factor.

CRediT authorship contribution statement

Kristen Dahl: Conceptualization, Methodology, Investigation, Formal analysis, Visualization, Writing – original draft, Writing – review & editing. **Joseph O'Malley:** Conceptualization, Funding acquisition, Resources, Supervision, Writing – review & editing. **Beverly Barnett: Conceptualization,** Methodology, Investigation, Resources, Writing – review & editing. **Bill Kline:** Conceptualization, Methodology, Investigation, Resources, Writing – review & editing. **Joseph Widdrington:** Resources, Methodology, Writing – review & editing.

Declaration of Competing Interest

The authors declare that they have no known competing financial interests or personal relationships that could have appeared to influence the work reported in this paper.

Data Availability

Data will be made available on request.

Acknowledgements

We would like to acknowledge Jed MacDonald, Francois Roupsard, and Simon Nicol for support in accessing and obtaining voucher samples from the Pacific Marine Specimen Bank, Thomas TinHan for support with coding and analyses in R, and Thomas Helser and Irina Benson for FT-NIR spectroscopy analysis support. We also thank two anonymous reviewers for their constructive reviews.

Author contributions

K. Dahl wrote the manuscript and conducted the analyses. J. O'Malley contributed to the study development and funding support. B. Barnett and B. Kline contributed to image analyses and performed FT-NIR spectroscopy scanning of all otoliths. J.B. Widdrington contributed to the selection of appropriate voucher samples and shipment. All authors provided editorial input to the final manuscript.

Appendix A. Supporting information

Supplementary data associated with this article can be found in the online version at doi:10.1016/j.fishres.2023.106927.

References

Anderson, W.D., 1981. A new species of Indo-West Pacific *Etelis* (Pisces: Lutjanidae), with comments on other species of the genus. Copeia 820–825.

Andrews, K.R., Fernandez-Silva, I., Randall, J.E., Ho, H.C., 2021. *Etelis boweni* sp. nov., a new cryptic deepwater eteline snapper from the Indo-Pacific (Perciformes: Lutjanidae). J. Fish. Biol. 99 (2), 335–344.

Andrews, K.R., Williams, A.J., Fernandez-Silva, I., Newman, S.J., Copus, J.M., Wakefield, C.B., Bowen, B.W., 2016. Phylogeny of deepwater snappers (Genus *Etelis*) reveals a cryptic species pair in the Indo-Pacific and Pleistocene invasion of the Atlantic. Mol. Phylogenetics Evol. 100, 361–371.

Bani, A., Poursaeid, S., Tuset, V.M., 2013. Comparative morphology of the sagittal otolith in three species of south Caspian gobies. J. Fish. Biol. 82 (4), 1321–1332.

Benson, I.M., Barnett, B.K., Helser, T.E., 2020. Classification of fish species from different ecosystems using the near infrared diffuse reflectance spectra of otoliths. J. Infrared Spectrosc. 28 (4), 224–235.

Cuvier, M.L.B., Valenciennes, M. (1828) Chapter VI. *Etelis*. In: Histoire naturelle des poissons. Tome II, Museum Histoire Naturelle, Paris, pp. 127–131.

Gaemers, P.A.M., 1984. Taxonomic position of the Cichlidae (Pisces, Perciformes) as demonstrated by the morphology of their otoliths. Neth. J. Zool. 34 (4), 566–595.

Helser, T.E., Benson, I.M., & Barnett, B. (2019b) Proceedings of the research workshop on the rapid estimation of fish age using Fourier Transform Near Infrared Spectroscopy (FT-NIRS). AFSC Processed Rep. 2019–06, 195 pp. Alaska Fish. Sci. Cent., NOAA, Natl. Mar. Fish. Serv., 7600 Sand Point Way NE, Seattle WA 98115.

Helser, T.E., Benson, I., Erickson, J., Healy, J., Kastelle, C.R., & Short, J.A. (2019a) A transformative approach to ageing fish otoliths using Fourier transform-near infrared spectroscopy (NIRS): a case study of eastern Bering Sea walleye pollock (Gadus chalcogrammus).

Kennard, R.W., Stone, L.A., 1969. Computer aided design of experiments. Technometrics 11 (1), 137–148.

Klecka, W.R. (1980) *Discriminant analysis* (Vol. 19) Sage.

Lachenbruch, P.A., Mickey, M.R., 1968. Estimation of error rates in discriminant analysis. Technometrics 10 (1), 1–11.

Langseth, B., Syslo, J., Yau, A., Carvalho, F., 2019. Stock assessments of the bottomfish management unit species of Guam, the Commonwealth of the Northern Mariana Islands, and American Samoa, 2019. NOAA Tech Memo. NMFS-PIFSC-86 177 (+ supplement, 165 pp.). doi:10.25923/bz8b-ng72.

Loeun, K.L., Goldstien, S., Gleeson, D., Nicol, S.J., Bradshaw, C.J., 2014. Limited genetic structure among broad-scale regions for two commercially harvested, tropical deep-water snappers in New Caledonia. Fish. Sci. 80 (1), 13–19.

Moore, B.R., Parker, S.J., Pinkerton, M.H., 2022. Otolith shape as a tool for species identification of the grenadiers *Macrourus caml* and *M. whitsoni*. Fish. Res. 253, 106370.

Murray, I., Williams, P., 1987. Chemical principles of near-infrared technology. In: Williams, P., Norris., K.H. (Eds.), Near Infrared Technology in the Agricultural and Food Industries. American Association of Cereal Chemists and The University of Wisconsin, Madison, WI., p. 330

Pacific Islands Fisheries Science Center. (2020) Life history program life history estimates. Available: https://inport.nmfs.noaa.gov/inport/item/59002. (July 2023).

Passerotti, M.S., Helser, T.E., Benson, I.M., Barnett, B.K., Ballenger, J.C., Bubley, W.J., Quattro, J.M., 2020. Age estimation of red snapper (*Lutjanus campechanus*) using FT-NIR spectroscopy: feasibility of application to production ageing for management. ICES J. Mar. Sci. 77 (6), 2144–2156.

Quinn, G.P., Keough, M.J., 2002. Experimental Design and Data Analysis for Biologists. Cambridge University Press.

R Development Core Team. (2014). R: A language and environment for statistical computing. R Foundation for Statistical Computing. Vienna, Austria. Retrieved from http://www.R-project.org.

Robins, J.B., Wedding, B.B., Wright, C., Grauf, S., Sellin, M., Fowler, A., Saunders, T., and Newman, S. (2015) Revolutionising fish ageing: using near infrared spectroscopy to age fish. Department of Agriculture, Fisheries and Forestry, Brisbane, April 2015. CC BY 3.0. 128 pp.

Smith, M.K., 1992. Regional differences in otolith morphology of the deep slope red snapper *Etelis carbunculus*. Can. J. Fish. Aquat. Sci. 49 (4), 795–804.

Smith, M.K., Kostlan, E., 1991. Estimates of age and growth of ehu *Etelis carbunculus* in four regions of the Pacific from density of daily increments in otoliths. Fish. Bull. 89 (3), 461–472.

Smith, N., Donato-Hunt, C., Allain, V., McKechnie, S., Moore, B. and Bertram, I. (2017) Developing a Pacific Community Marine Specimen Bank. 10th SPC Heads of Fisheries Meeting. 5 pp.

Solo 8.9.2 (2021) Eigenvector Research, Inc., Manson, WA USA 98831; software available at http://www.eigenvector.com.

Vance, C.K., Tolleson, D.R., Kinoshita, K., Rodriguez, J., Foley, W.J., 2016. Near infrared spectroscopy in wildlife and biodiversity. J. Infrared Spectrosc. 24 (1), 1–25.

Wakefield, C.B., Williams, A.J., Newman, S.J., Bunel, M., Dowling, C.E., Armstrong, C.A., Langlois, T.J., 2014. Rapid and reliable multivariate discrimination for two cryptic Eteline snappers using otolith morphometry. Fish. Res. 151, 100–106.

Wakefield, C.B., Williams, A.J., Fisher, E.A., Hall, N.G., Hesp, S.A., Halafihi, T., Newman, S.J., 2020. Variations in life history characteristics of the deep-water giant ruby snapper (*Etelis* sp.) between the Indian and Pacific Oceans and application of a data-poor assessment. Fish. Res. 230, 105651.

Wedding, B.B., Forrest, A.J., Wright, C., Grauf, S., Exley, P., Poole, S.E., 2014. A novel method for the age estimation of saddletail snapper (*Lutjanus malabaricus*) using Fourier transform-near infrared (FT-NIR) spectroscopy. Mar. Freshw. Res. 65 (10), 894–900.

White, J.W., Ruttenberg, B.I., 2007. Discriminant function analysis in marine ecology: some oversights and their solutions. Mar. Ecol. Prog. Ser. 329, 301–305.

Williams, A.J., Loeun, K., Nicol, S.J., Chavance, P., Ducrocq, M., Harley, S.J., Bradshaw, C.J.A., 2013. Population biology and vulnerability to fishing of deep-water Eteline snappers. J. Appl. Ichthyol. 29 (2), 395–403.

Williams, A.J., Newman, S.J., Wakefield, C.B., Bunel, M., Halafihi, T., Kaltavara, J., Nicol, S.J., 2015. Evaluating the performance of otolith morphometrics in deriving age compositions and mortality rates for assessment of data-poor tropical fisheries. ICES J. Mar. Sci. 72 (7), 2098–2109.

Williams, A.J., Wakefield, C.B., Newman, S.J., Vourey, E., Abascal, F.J., Halafihi, T., Nicol, S.J., 2017. Oceanic, latitudinal, and sex-specific variation in demography of a tropical deepwater snapper across the Indo-Pacific region. Front. Mar. Sci. 4, 382.

Zischke, M.T., Litherland, L., Tilyard, B.R., Stratford, N.J., Jones, E.L., Wang, Y.G., 2016. Otolith morphology of four mackerel species (*Scomberomorus* spp.) in Australia: Species differentiation and prediction for fisheries monitoring and assessment. Fish. Res. 176, 39–47.